京都大学防災研究所年報　第45号B-2　平成14年４月
Annuals of Disas. Prev. Res. Inst., Kyoto Univ., No.45B-2, 2002

Velocity Measurements in Open Channel Flow with Rectangular Embayments Formed by Spur Dykes

MUTO Yasunori, BABA Yasuyuki and AYA Shiro*

* Department of Civil Engineering, Osaka Institute of Technology

Synopsis

Velocity measurements are conducted in open channel flow with rectangular embayments. The measurements were carried out both in a real river and in a laboratory flume. The large-scale PIV (LSPIV) method was adopted for the field measurements, whereas a 2-D electromagnet current meter (ECM) was used in the laboratory measurements. Behaviour of large-scale circulation flow induced in the embayments is the main concern. Factors giving instability on the circulation flow is also discussed.

Keywords: velocity measurements; embayment; field measurements in a river; laboratory experiments; LSPIV; large-scale circulation

1. Introduction

In many Japanese major rivers running on an alluvial plain, spur dykes for maintaining navigation course had been constructed for more than 100 years. Nowadays, as inland navigation declined, spur dykes for this purpose are no longer newly installed in such a river reach, however the dykes constructed in the old age still remain in several rivers and the spaces between these dykes show a new function for the rivers, mainly from the ecological point of view. The spaces, a sort of embayment and called “wando” in Japanese, are recognised to possess a precious closed ecosystem within it and provide preferable environment for natural lives, and thus should be preserved and passed onto the next generation in a good condition. There also exist several rivers in which spur dykes, or “wando”, have been newly constructed in the last decade. In these rivers the dykes no longer have the old function, but are expected to show the aforementioned new function, i.e. create a good habitat for natural lives there.

As for the hydraulics in the embayment, it is generally known that velocity is slow and water quality is stable compared with those in the main flow region, and sediment tends to be deposited, which leads the embayment to become shallower. It is, however, quite recent that flow characteristics in the embayment and its related problems began studied in a truly academic meaning. Kimura et al. (1994 & 1995) studied free surface oscillation and fluid exchange in and around a rectangular embayment. Furthermore they (1998) studied behaviour of suspended sediment within the embayment. Nakagawa et al. (1995) measured velocity distributions in and around an embayment under flooding conditions. Ikeda et al. (1999), Wallast et al. (1999) and Uijttewaal et al. (2001) studied flow exchange in groyne fields, which has some similarities to embayments. By these researches the hydraulics in the embayment have gradually been clarified, but its whole picture is still not clear. One of the reasons is that many parameters are related to the problem, thus investigation, either numerically or

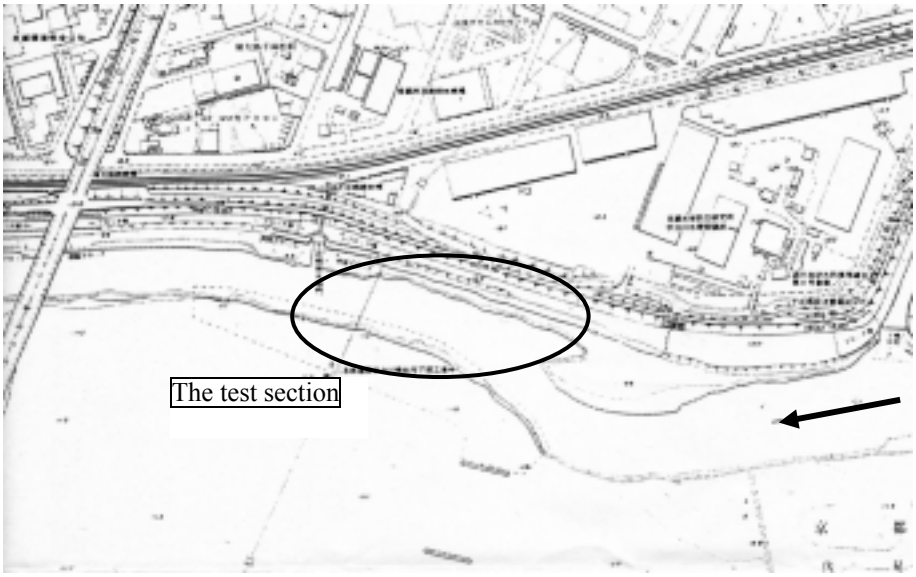

Fig. 1 The test section in the field measurements : 42.7kp-42.9kp of the Yodo River

experimentally, should be carried on rather systematically.

The authors (2000a & 2000b) from this point of view conducted some experiments on the flow in an embayment. The selected parameters were the aspect ratio of the embayment and the flooding depth. The effects of these parameters on flow patterns could successively be drawn by measuring velocity distribution in detail using laser Doppler anemometers (LDA) and an electromagnetic current meter (ECM). Turbulence characteristics at the interface between the embayment and the main flow region were also clarified and the results firmly support the fact that the flow exchange takes place more effectively for the embayment of the larger aspect ratio within the selected range.

On the basis of the information obtained from the above experiments, further investigation was carried out in a real river. In the test section four spur dykes form three embayments on the one side of a river along a nearly straight reach. A similar geometry was modelled in a straight laboratory flume. Velocity measurements were performed by the large-scale PIV (LSPIV) method in the river and by an electromagnet current meter in the laboratory. Flow structure in the embayments is appreciated from the mean flow analyses in conjunction with the scale effect.

2. Field Measurements

2.1 The test section

The Yodo River, located in the central part of Japan, runs from Lake Biwa, the biggest lake in

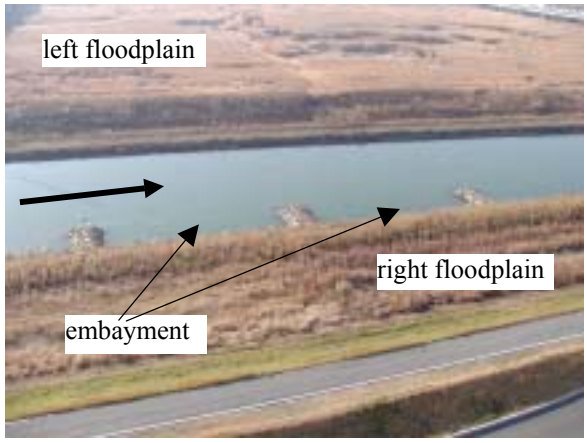

Fig. 2 Overview of the test section in the field measurements. (the 2nd & 3rd embayments)

Japan, and goes through Kyoto and Osaka, two of the biggest cities of the country, into Osaka Bay. Length of the main river is only 75km, however it has many big tributaries, also including the lake itself, thus its watershed area is 8240km^2, rather large compared with its length. The test section is situated on the south end of Kyoto City, and is about 42.8km from the river mouth (see Fig. 1). The test section has a compound cross section, a deeper main channel along the centre and shallower flood plains on both sides. Total width of the river in the test section is over 600m, and the main channel width is about 60m. The channel bed slope is the order of 10^{-4}. There exist four rock dykes only on the righthand side of the main channel along nearly a straight reach. Each dyke extends about 10m perpendicular from the channel side toward the main stream. Longitudinal distance from one dyke to the next is about 40m.

Fig. 3 The tracer and its application in order to visualise the surface flow

Thus three embayments whose aspect ratio is 4 are formed along the righthand side of the channel (see Fig. 2). Velocity measurements were carried out in the 2nd and 3rd embayments. Measurements in the 1st embayment were not attempted, since an upstream bend section and a large bridge pier located in that section clearly affect flow structure in this embayment. The flow discharge during the measurements was 52.2 to 57.7m^3/s and the averaged water depth was 2.8m. The Reynolds number is the order of 10^6 and the Froude number is 0.08.

2.2 Flow visualization technique

In the field measurements flow pattern on the water surface was visualised with the aid of solid tracers. The tracer is cylindrical, 7cm length and 2cm diameter, and hollow. The specific gravity is about 0.1. Its main ingredient is PVOH and cornstarch. The tracer, when thrown into water, floats on the surface at first, then it starts to absorb the ambient water and to sink, and finally dissolves in water within 5 minutes (see Fig. 3). It is biologically degradable and thus no damage on water quality and the environment of the river.

Path lines of the tracers were captured by a digital video camera (SONY DCR-TRV30). The camera was set on the 40m-height station of the 55m meteorological observation tower at Ujigawa Hydraulics Laboratory, Kyoto University (see Fig. 4). The laboratory is just located on the north side of the test section, and the horizontal distance between the test section and the tower is about 100m. Oblique angle of the camera axis was thus about 20 degree. Recording speed of the video camera is 30 frames per second.

Fig. 4 The observation tower

2.3 Picture processing and PIV techniques

In order to obtain good velocity data from the captured images, there need two processes. One is removing image distortion, and the other is so-called PIV processing. The image distortion is brought by the lens of the camera, large distance between the flow field and the camera, and the oblique angle between the camera axis and the flow field plane. The distortion due to these factors is removed using a geometry transformation technique. The PIV processing is essentially the same as that of conventional PIV. Only the differences between large-scale PIV (LSPIV) and conventional PIV are that the target flow field is rather large (herein 50m × 40m = 2000m^2) and there is no free selection on light, nor can expect support of high intensity light like laser in the laboratory, which may yield less contrast on the images. LSPIV, thus, may need enhancement of the captured images. These pre-processing on the images and PIV processing are executed on the self-developed software.

Further information as to the processing and the software algorithm can be found in detail elsewhere in Fujita et al. (1997 & 1998).

2.4 Results

Figure 5a shows an example of the original image recorded on the videotape. In this figure 400 frames, selected every 10 frames (0.333sec. interval) from the original consecutive frames on the tape, are overlaid. By doing this path lines, and flow patterns in the duration of 133 seconds as a result, can be recognised

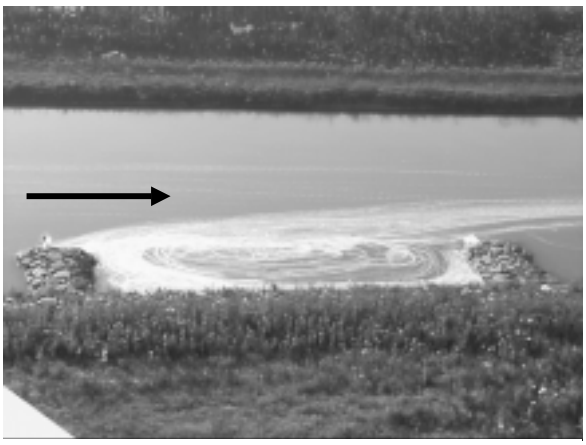

Fig. 5a An example of flow visualisation (original image)

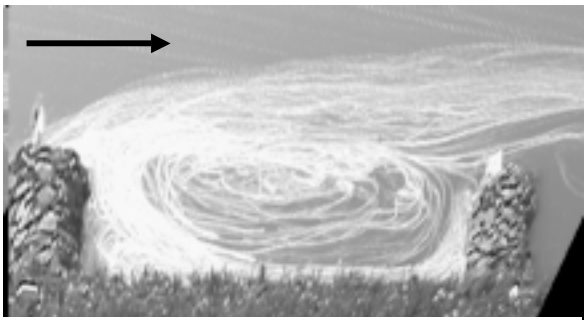

Fig. 5b An example of flow visualisation (adjusted image by geometry transformation technique)

in the figure. A large circulating flow induced in the embayment can be seen, however the camera angle, i.e. the image, is rather distorted due to the aforementioned factors. Figure 5b shows the adjusted image of that in Fig. 5a, transformed onto a plane parallel to the flow field. Some portions of the original image are discarded in order to increase processing accuracy in the following PIV. Reliability of the transformation is checked by the dimensions of geometry in the adjusted image, such as the aspect ratio of the embayment, and it can be acceptable. Further processing as to PIV has been done using such transformed images.

Figure 6 shows a typical flow pattern in the 2nd embayment and its variation within 2 minutes. Each image is obtained by overlaying 90 frames, i.e. for 30 seconds record, in the same manner as in Figure 2. It can be seen in the figure that a large clockwise circulation is formed within the embayment. The circulation bulges out into the main flow region to some extent. In the last image a counter small cell is also recognised in the left bottom corner. It can be said from these figures that a large circulation fairly stably exists in the embayment. Once it covers most of its area it remains for over 2 minutes and during

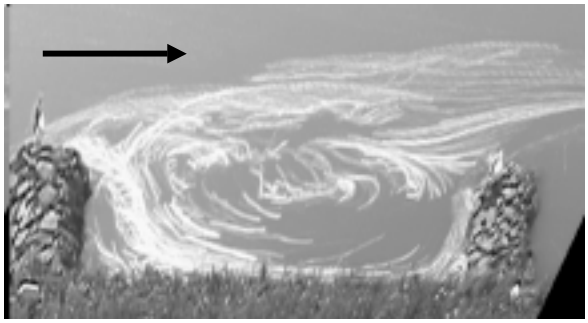

(a. t = 0’00” – 0’30”)

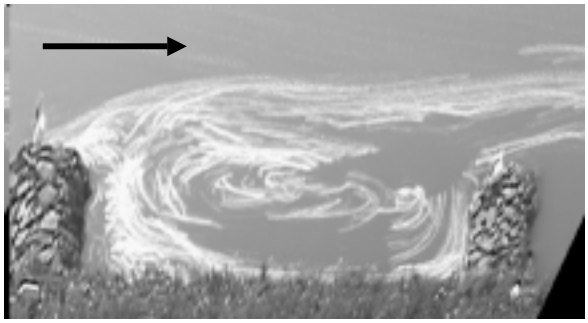

(b. t = 0’30” – 1’00”)

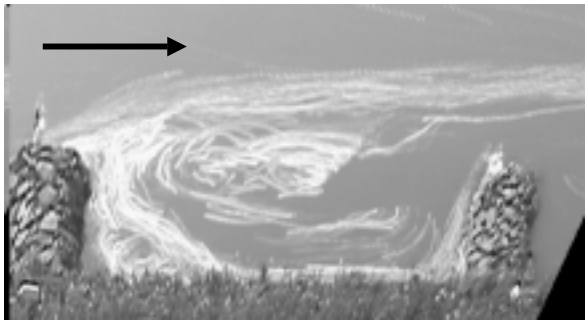

(c. t = 1’00” – 1’30”)

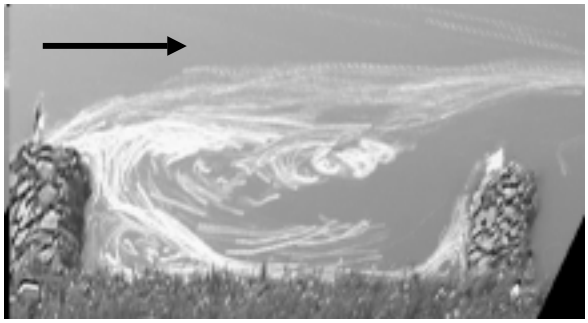

(d. t = 1’30” – 2’00”)

Fig. 6 Flow patterns in the 2nd embayment of the field (t = 0’00” – 2’00”)

that time it works as if it protects the main flow intruding into the embayment. However, this large circulation is not always dominant. The other flow pattern observed in the same embayment is shown in Fig. 7. In this figure it is seen that the size of the large circulation is reduced and its shape is distorted, and the bulge toward the main flow region cannot be seen. In such a situation the main flow enters into the embayment. It is clear that the flow around the

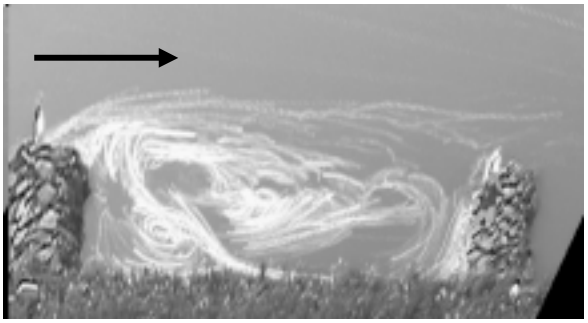

(a. t = 3'30" – 4'00")

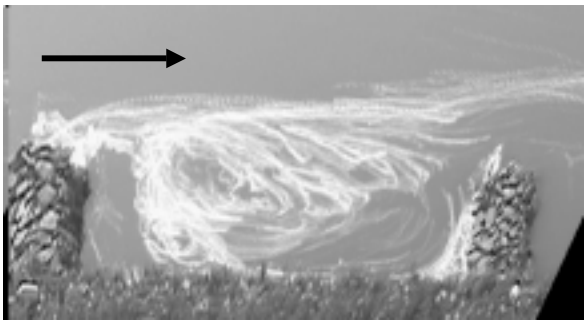

(b. t = 4'30" – 5'00")

Fig. 7 Flow patterns in the 2nd embayment of the field (t = 3'30" – 5'00")

interface changes its direction laterally, particularly on the downstream side of the embayment, compared Fig. 6 with Fig. 7. This indicates that flow exchange is closely related with the behaviour of circular flow in the embayment.

Figure 8 shows velocity vectors calculated from the video images via LSPIV technique (in this figure the vectors are plotted in the upside-down manner against Figs. 6 & 7, for the comparison purpose with the experimental results shown later in this paper: and this is also applied to Fig. 10). As is the same as a conventional PIV, two frames are used to calculate one data set of vector field. Time lag of the frames was 0.667sec. (20 frames). 21 × 11 = 231 points were set as the calculation grid in the processing area. 199 data set were calculated and averaged for each plotting, although some erroneous data were discarded before averaging (see Fujita et al. 1998). Figure 8a was obtained using the same frame set as shown in Fig. 6, whereas Fig. 8b using the other set including the images shown in Fig. 7. In Fig. 8 the difference of the flow pattern can be seen much clearer. Induced velocity on the outer edge of the circular flow is similar, about 25cm/s which is 25% of the main flow velocity in magnitude. However, a stagnant area formed around the core of the circulation is different both in size and position, which may influence sediment deposition in the embayment. In fig. 8b the faster flow from the main

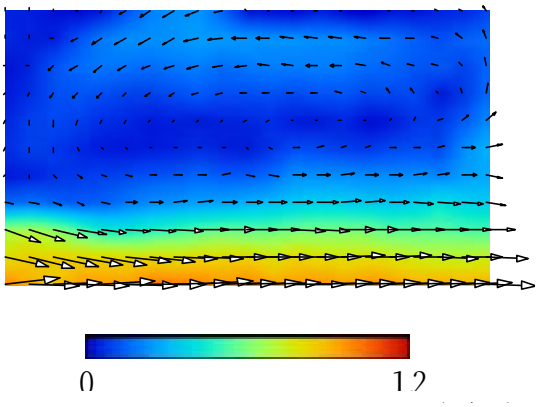

Fig. 8a Velocity vectors in the 2nd embayment of the field, averaged over t = 0'00" to 2'13"

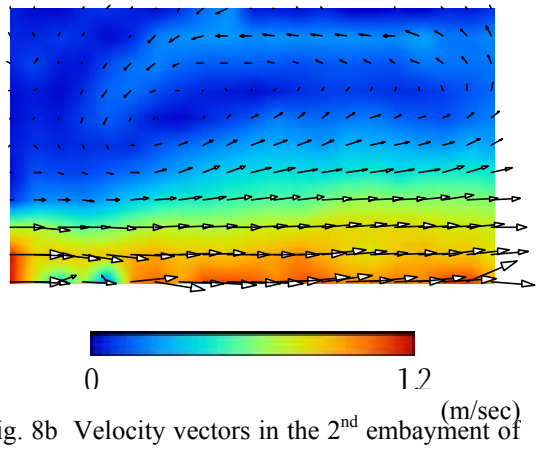

Fig. 8b Velocity vectors in the 2nd embayment of the field, averaged over t = 3'30" to 5'43"

flow region largely enters into the embayment on the downstream side. The affected area by the faster flow is contrarily a stagnant area in Fig. 8a, which means that velocity fluctuates dynamically, and thus sediment movement in this area is also very complicated. Overall, it can be said for the 2nd embayment that there exists large-scale fluctuation whose period is over 2 minutes, one term for the data set. The whole picture of flow behaviour may not be caught by such a short time.

The results for the 3rd embayment are shown in Figs. 9 & 10, in the same manner as for the 2nd embayment in Figs. 6-8. For the 3rd embayment the large-scale fluctuation seen in the 2nd embayment cannot be seen. As can be seen in Fig. 9 a relatively stable flow pattern is observed. The vector plotting in Fig. 10, on the other hand, shows a quite different pattern from that in Fig. 8. It seems for this embayment that there exist two cells of having different axes, a large cell, occupying nearly the whole area, bearing inside the other elliptic small cell, which is located at the upstream half near the

interface. Velocity induced on the edge of the large cell is about 30cm/s, slightly faster than that for the

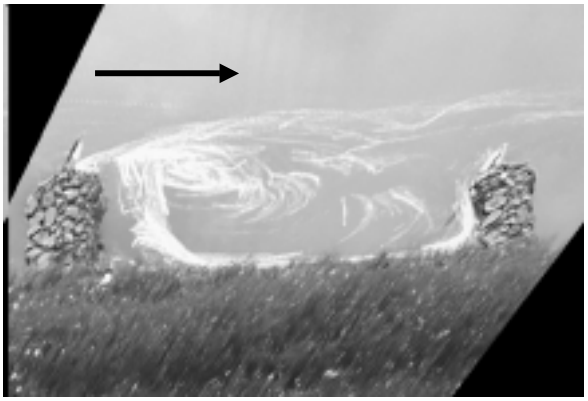

(a. t = 0'00" – 0'30")

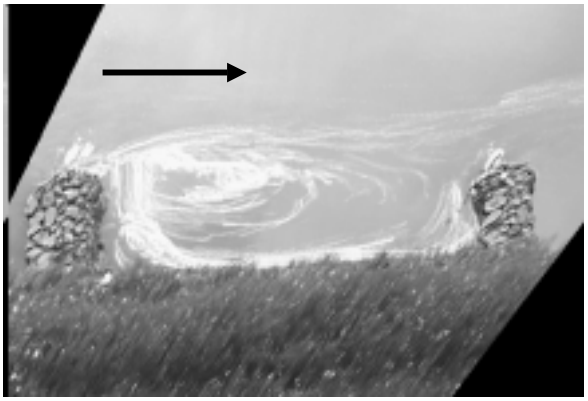

(b. t = 0'30" – 1'00")

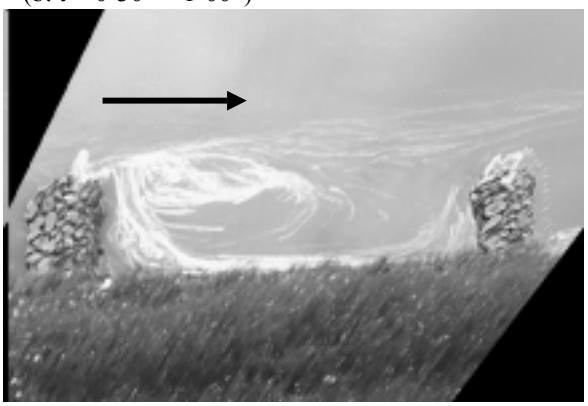

(c. t = 1'00" – 1'30")

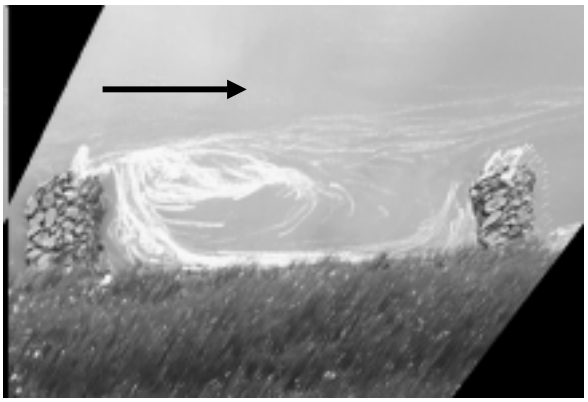

(d. t = 1'30" – 2'00")

Fig. 9 Flow patterns in the 3rd embayment of the field (t = 0'00" – 2'00")

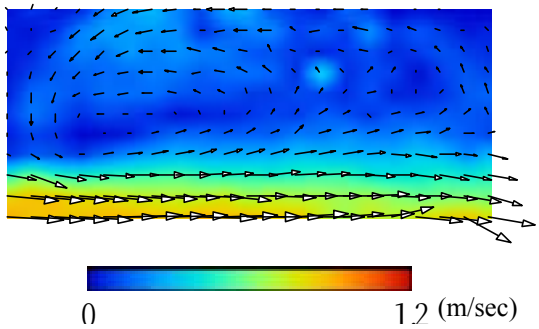

Fig. 10 Velocity vectors in the 3rd embayment of the field, averaged over t = 3'30" to 5'43"

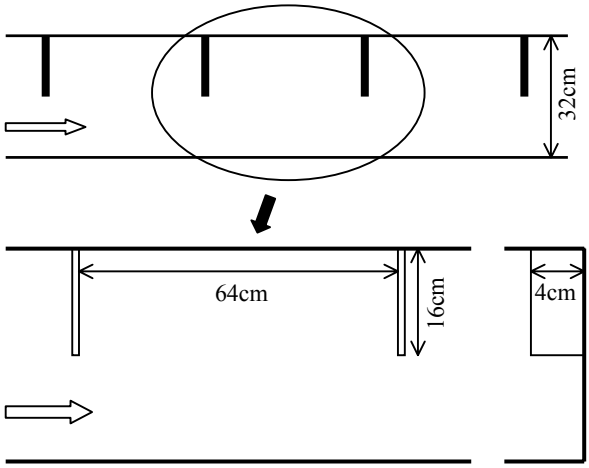

Fig. 11 Channel geometry for the laboratory experiments, top: the test section, bottom: a model embayment with spur dykes

2nd embayment. It should be noted that the stagnant area is formed quite differently, and as a result sediment movement and bed deformation in this embayment can also be different from the foregoing embayment.

3. Laboratory Experiments

3.1 Experimental set-up

The laboratory flume is made of glass and has 8m long, 32cm wide, 25cm deep and its slope of 0.00125. Four model spur dykes, each of them has dimensions of 16cm long and 4cm height, were set along the one side of the flumes and three model embayments attached to the main channel were formed in the middle of the flumes. Each model dyke was set with distance of 64cm, thus the aspect ratio of the embayment was 4, the same as that of the field

measurements. The test section including the model embayments was about 2m long, set about 2m upstream from the end of the channel. Schematic

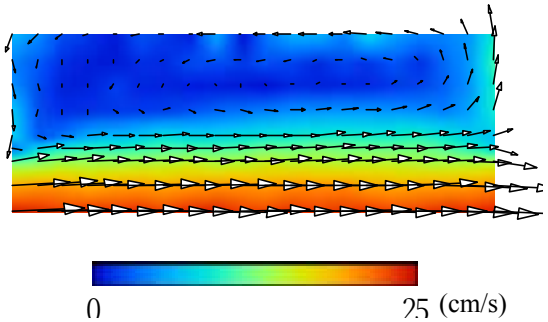

Fig. 12a Velocity vectors in the 2nd embayment of the experimental flume measured by ECM

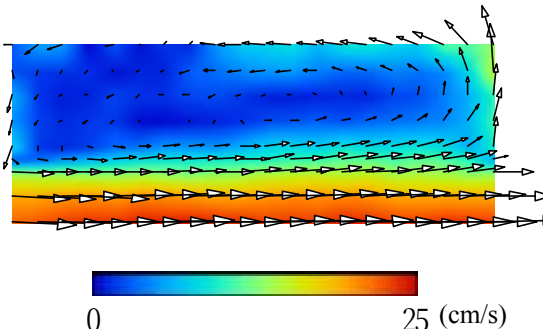

Fig. 12b Velocity vectors in the 3rd embayment of the experimental flume measured by ECM

view of channel geometry and definition of dimensions are shown in Fig. 11.

The hydraulic condition for the velocity measurements was as follows: the flow discharge, Q = 1.37liter/s, the water depth, h = 3.8cm, the discharge velocity, v = 11.3cm/s, the Reynolds number, Re = 4280 and the Froude number, Fr = 0.18.

For velocity measurements a 2-component electromagnetic current meter was used and the streamwise and lateral components of velocity were measured simultaneously. The measurement grid of 180 points (20 × 9) was set in each embayment. Sampling rate for one point was 10Hz and 300 data was collected for each point. The measurements were carried out in the 2nd and 3rd embayments, for the comparison with the results of the field measurements.

3.2 Results

The results of point measurements of velocity for both embayments are shown in Fig. 12 in a vector form. It can be seen that the basic flow pattern is

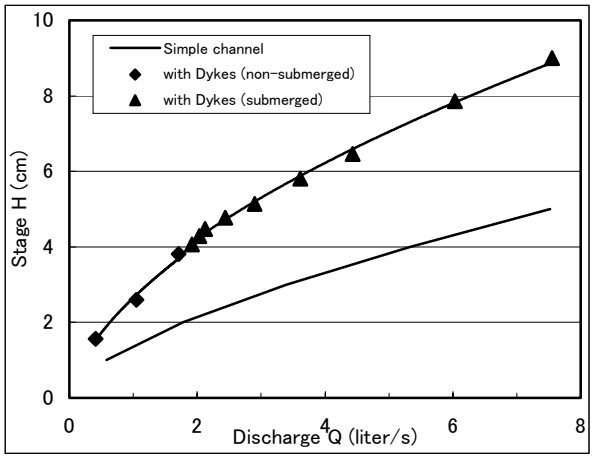

Fig. 13 Stage-discharge relationships for the simple rectangular channel with and without dykes

quite similar in these embayments. Just one large cell of anticlockwise circulation is formed and it occupies nearly the whole area of the embayment. The core, or the vertical axis, of the cell is located in the downstream half of the embayment. Another counter cell with clockwise circulation, which sometimes appears in the upstream top corner, cannot be clearly seen. According to the experiments by Nezu et al. (2001), the large cell becomes more elliptic and the core of the cell approaches the interface, when the aspect ratio of the embayment increases from 3 to 5. The results herein, however, do not seem to follow such tendencies, rather, are similar to those for the aspect ratio of 3 (see also Muto et al. 2000a). It should be noted that the boundary condition at the upstream end is different between the experiments herein and the literatures. The experimental flumes in the literatures were both a compound cross section, which can possibly bring a different flow structure in the embayment.

Resistance effect of spur dykes on channel conveyance capacity is most easily and directly estimated by examining stage-discharge relationship. The stage-discharge relationships for the tested channel are shown in Fig. 13. In the figure the experimental results are plotted as dots and the lines are drawn just to help reader's eye. The other line referred to as "Simple channel" is the stage-discharge curve without dykes, calculated by Manning's equation with n=0.011. It can be seen in the figure that, with dykes, the increments of the curve drastically change at the height of the dyke, 4cm. This change of the increment is so-called compound channel effect. In fact there is no flood plain, however the dykes play the same role as the flood plain regarding this function. The figure also clearly

shows that resistance due to the spur dykes is quite large. Due to the existence of the dykes the discharge is reduced up to about 40% of the simple channel case when comparing at the same stage. This can be understood judging from the velocity distributions shown in Fig. 12, since effective channel width is reduced a lot, due to the dykes and the circulation flow induced behind the dykes. As was shown in 2.4, the circulation flow has some instability from one room to another in the field. In such a case resistance due to the circulation flow may sometimes work more effectively, as in which the circulation bulges towards the main flow region.

4. Discussions

It has been pointed out in the literatures that the aspect ratio of the embayment is the most important determinant of the circular flow induced there (see e.g. Nakagawa et al. 1995, Muto et al. 2000). In other words it is expected that, if the aspect ratio is the same, the flow structure as to the circular cells should also be similar. The model embayment was designed on the basis of this conjecture. However, when comparing the results of the field measurements and the laboratory experiments shown in the previous chapters, they may give somewhat different impressions, despite the same aspect ratio of 4 (see e.g. Figs. 8, 10 & 12).

First of all, the measuring methods were different between the field and the laboratory. The Eulerian method adopted in the laboratory (point-velocity measurements) basically cannot draw square information like the fluctuation of vortical motion. However, if the flow is steady and data is long enough, the averaged results should be the same either raw data are recorded by the Eulerian or the Lagrangian. One can also be noticed that the measured plane was different, on the surface for the fields whereas at the half depth for the laboratory. This difference, however, has already been checked not to yield much difference, since the flow within the embayment is assumed 2-D condition and thus should be homogeneous dynamically except quite close to the bottom.

As mentioned in 2.4, flow patterns between the 2nd and 3rd embayments are more or less different in the field measurements, however such difference cannot be seen for the experimental results. This means that the difference is not brought due to the position in consecutive embayments. In the field measurements the upstream reach of the test section slightly bends, as was pointed out in 2.1. The course of the flow out of the bend section sometimes staggers, and in case hitting the top of the 2nd groyne it goes directly into the 2nd embayment (see Fig. 7). This explains that, although the bend does not seem so much, such geometry irregularity strongly affect the flow structure. The reason why a unique small cell is formed in the 3rd embayment is still not clear. In addition to the effect of mutual interference between two embayments, this could also be attributed to the geometry irregularity such as bed undulation.

Finally properties of the dominant circulation should be discussed. Most distinct point is the position of the core, in the laboratory being located in the downstream half and inside of the embayment, whereas in the field being in the upstream half and more close to the interface. In addition, the maximum edge speed of the cell relative to the main flow is generally faster in the field, about 25%, than in the laboratory, about 17%. Here one can recognise some similarity between the embayment and sudden expansion in geometry. Because both have a sudden expansion reach, in which a large, stable and strong circular flow is induced. It is deemed that the mechanism inducing the circular cells is similar, and such vortical motion is basically determined by the Reynolds number. Thus, apart from the geometry irregularity considered above, the Reynolds number is the most important parameter in describing the phenomenon. In order to clarify this feature, known as the scale effect, further data acquisition, as well as data analyses, is still undergoing.

5. Conclusions

The summary of the paper can be given as follows:

- Field measurements were carried out in a real river by means of a flow visualisation technique. LSPIV method can successively draw velocity fields in and around embayments in the river.
- Laboratory experiments were conducted in a simplified model of the river reach where the field measurements were carried out. Velocity distribution in the embayments whose aspect ratio (AR) is 4, adopted herein, is similar to that of AR = 3 in the literatures.
- Some factors affected the differences of flow patterns between the field and the laboratory were discussed. The difference of the geometry irregularity and Reynolds number can be the main causatives.

- Stage-discharge relationship was examined with the laboratory data and spur dykes working as a roughness element was estimated. For the case with the dykes the discharge is reduced up to about 40% of the simple channel case when comparing at the same stage.
- Further data acquisition is strongly needed, especially for the filed measurements, which will brush up the reliability of both the LSPIV method and the data itself, and is expected to give new insight into this kind of flow.

Acknowledgement

The authors would like to thank Dr. Fujita I., Research Center for Urban Safety and Security, Kobe University, for his advice in the application of the LSPIV method. The authors would also like to thank Mr. Kitagawa Y., Ujigawa Hydraulics Laboratory, DPRI, Kyoto University, for his cooperation in the field measurements. Help and guidance of the field measurements by Yodogawa Public Work Office, MLIT, should also be acknowledged.

References

Fujita, I., Aya, S. & Deguchi, T. (1997): Surface velocity measurement of river flow using video images of an oblique angle. *Proc. 27th IAHR Cong., San Francisco, USA*, Vol.B, No.1, pp.227-232.

Fujita, I., Muste, M. & Kruger, A. (1998): Large-scale particle image velocimetry for flow analysis in hydraulic engineering applications. *J. Hydr. Res.*, Vol.36, No.3, pp.397-414.

Ikeda, S., Yoshiike, T. & Sugimoto, T. (1999): Experimental study on the structure of open channel flow with impermeable spur dikes. *Annual J. of Hydr. Engrg., JSCE*, Vol.43, pp.281-286. (in Japanese)

Kimura, I., Hosoda, T. & Tomochika, H. (1994): Characteristics of unsteady flow behaviour in the open channel with rectangular dead zone. *Proc. Hydr. Engrg., JSCE*, Vol.38, pp.425-430. (in Japanese)

Kimura, I., Hosoda, T., Muramoto, Y. & Yasunaga R. (1995): Fundamental properties of free surface oscillation in dead zone of open channel flows. *Annual J. of Hydr. Engrg., JSCE*, Vol.39, pp.779-784. (in Japanese)

Kimura, I., Hosoda, T. & Muramoto, Y. (1998): Characteristics of suspended sediment transport in open channel flows with a dead zone. *Annual J. of Hydr. Engrg., JSCE*, Vol.42, pp.1057-1062. (in Japanese)

Muto, Y., Imamoto, H. & Ishigaki, T. (2000a): Turbulence characteristics of a shear flow in an embayment attached to a straight open channel. *Proc. 4th Int'l Conf. on Hydroscience and Engrg., Seoul, Korea*, p.232.

Muto, Y., Imamoto, H. & Ishigaki, T. (2000b): Velocity measurements in a straight open channel with a rectangular embayment. *Proc. 12th APD-IAHR, Bangkok, Thailand*.

Nezu, I., Onitsuka, K. & Takahashi, S. (2001): Turbulence characteristics and coherent vortices in open-channel flows with a horizontally dead zone. *J. Hydr., Coastal and Envir. Engrg., JSCE*, No.684/II-56, pp.11-20.

Nakagawa, K., Kawahara, Y. & Tamai, N. (1995): Experimental study on hydraulic characteristics of flows in embayments. *Annual J. of Hydr. Engrg., JSCE*, Vol.39, pp.595-600. (in Japanese)

Uijttewaal, W.S.J., Lehmann, D. & Mazijk, A. van. (2001): Exchange process between a river and its groyne fields: model experiments. *J. Hydr. Engrg.*, Vol.127, No.11, pp.928-936.

Wallast, I., Uijttewaal, W.S.J. & Mazijk, A. van. (1999): Exchange processes between groyne field and main stream. *Proc. 28th IAHR Cong., Graz, Austria*, p.232.

要　旨

水制によって形成される開水路死水域内の速度分布を，現地観測および室内実験により計測した．現地観測では，環境影響負荷に配慮したトレーサを用いた表面流況可視化を行い，Large-scale ＰＩＶ（ＬＳＰＩＶ）法により速度分布を得た．室内実験では，２成分電磁流速計による点計測を行った．その結果，室内実験では明確でない循環流の不安定性が現地では見られた．この不安定性は，地形の不規則性，上流条件の不安定性の履歴によりもたらされる他，レイノルズ数による影響も考慮される．

キーワード：速度計測，水制，死水域，現地観測，室内実験，ＬＳＰＩＶ法，循環流